CHARACTERISTIC FEATURES OF THE FLUIDIZED BED BOILER STARTING

Eugeni Pitsukha[1*], Yury Teplitski[1], Alexander Roslik[1], Rafail Isemin[2], Dmitry Klimov[2], Alexander Mikhalev[2], Valentin Borodulya[1], Vitaly Dubina[3]

[1]*A.V. Luikov Heat and Mass Transfer Institute, 15 Brovka Str., 220072, Minsk, Belarus*

[2]*Tambov State Technical University, 106 Sovetskaya Str., 392000, Russia*

[3]*Specialized Design Office for Complex Microclimate Equipment, 66 Smirnov Str., 224014, Brest, Belarus*

*Email: *pit.ea@mail.ru*

The process of heating the granular bed under the conditions of thermal fluidization by heat supply through its upper boundary and through the gas distributor was studied.

INTRODUCTION

The problem of burning solid biofuels in the fluidized bed boilers draws much attention due to undoubted advantages of this method comparing to the traditional ones.

One of the problems today is seamless in operation a start-up heating boiler. Ignition can be realized by various methods (Chermalyh G. N., Mahorin K. E., 1965; Keler V. R. et al., 1989; Protsailo M. Y. et al. 1991; Ruzhnikov S. G. et al. 1988; Shteiner I. N. et al. 1985; Zabrodski S. S., 1971). Typically, inert bed material preheated in any way to the ignition temperature of the fuel, and only then the fuel is supplied to the working place. The simplest ignition is performed using the fuel gas, which is burned in a gas burner under of the gas distribution grid (lower heating) or over the bed (upper heating). In both cases, the filtering gas in the process of kindling carries away a considerable amount of heat, which does not allow complete heating bed in a short enough time. Reduce these losses it allows starting when the bed is fixed initially and become fluidized during the heating. Such process can be called thermal fluidization. The purpose of this work is to study it in the combined heating, blending together upper and lower heating of inert material bed.

FORMULATION OF THE PROBLEM

The model of thermal fluidization, based on the description of the propagation of the front of a strong discontinuity due to the jump in the longitudinal thermal conductivity coefficient in the fixed bed – fluidized bed transition is using for the process of heating the granular bed description (Pitsukha E. A. et al., 2016):

$$c_s\rho_s(1-\varepsilon)\frac{\partial T_{gb}}{\partial t}+c_f J_f\frac{\partial T_{gb}}{\partial x}=\lambda_{gb}\frac{\partial^2 T_{gb}}{\partial x^2}, \qquad 0\le x<h(t), \tag{1}$$

$$T_{fb}=T_{mb}, \qquad h(t)<x\le H; \tag{2}$$

boundary conditions:

$$t=0, \qquad T_{gb}=T_0, \qquad h(0)=H, \tag{3}$$

$$x=0, \qquad c_f J_f(T^0-T_{gb})=-\lambda_{gb}\frac{\partial T_{gb}}{\partial x}, \tag{4}$$

$$x=h, \qquad -c_s\rho_s(1-\varepsilon)(T_{mb}-T_{mf})\frac{dh}{dt}=Q-\lambda_{gb}\frac{\partial T_{gb}}{\partial x}-c_f J_f(T_{mb}-T_{mf}). \tag{5}$$

Condition (5) is formulated for the case of $Q\ge c_f J_f(T_{mb}-T_0)$, taking into account the effect of heat carried away from the bed, and describes the movement of the front "fixed bed – fluidized bed" transition. The temperature in the front is T_{mb}, corresponding to the minimum bubbles formation velocity u_{mb} (Richardson J. F., 1974). At lower heat fluxes, which are insufficient for the fluidization of the bed on the upper border ($x = H$) the condition

$$x = H, \qquad \lambda_{gb} \frac{\partial T_{gb}}{\partial x} = Q \tag{6}$$

has to be used instead of (5). Note that with assuming $T^0 = T_0$ one has upper heating, and for the $Q = 0$ – lover heating having a Dankverts boundary condition:

$$x = H, \qquad \frac{\partial T_{gb}}{\partial x} = 0 . \tag{7}$$

RESULTS

The method of solution of (1) – (7) is shown in (Pitsukha E. A. et al., 2016). Fig. 1 and 2 show the spatial and temporal distributions of the bed temperature for $T^0 < T_{mb}$. In these circumstances, the front of "fixed - fluidized bed" transition (x=h) passes through all height of granular bed (Fig 1.) during a time interval determined by the balance equation:

$$\tau_{fb} = \frac{c_s \rho_s (1-\varepsilon) H (T_{mb} - T_0)}{Q - c_f J_f (T_{mb} - T^0)} \tag{8}$$

and starting from the time t_* (Fig. 1c), whereby for any $x < h(t_*)$ holds $T_{gb}(x) = T^0$, one has an upper heating bed process with temperature T^0 before the front.

With $t > \tau_{fb}$ (Fig. 2) the fluidized bed continues to be heated in accordance with the equation

$$c_s \rho_s (1-\varepsilon) \frac{dT_{fb}}{dt} = Q - c_f J_f (T_{fb} - T^0) , \tag{9}$$

which implies a perfect mixing of the particles.

The solution of the (9) provided

$$t = \tau_{fb}, \qquad T_{fb} = T_{mb} \tag{10}$$

has a kind of

$$T_{fb} = T^0 + \frac{Q}{c_f J_f} + \left(T_{mb} - (T^0 + \frac{Q}{c_f J_f}) \right) \exp\left(- \frac{c_f J_f (t - \tau_{gb})}{c_s \rho_s (1-\varepsilon) H} \right). \tag{11}$$

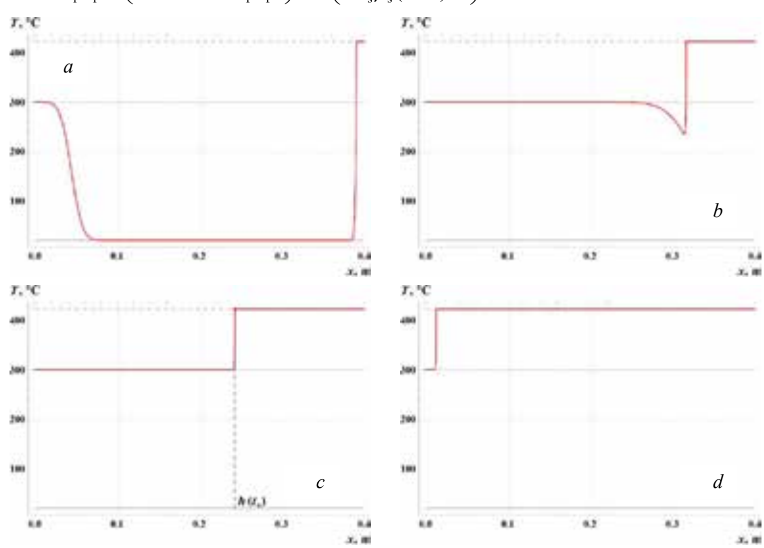

Fig. 1. Temperature distributions along the bed height in different time moments. T^0 = 300 °C, τ_{fb} = 1800 s. (0.1·τ_{fb} (a), 0.75·τ_{fb} (b), t_* = 1450 s (c), 0.99·τ_{fb} (d)). H = 0.4 m, d = 1.1·10^{-3} m, ε = 0.5, c_s = 800 J/(kg·K), c_f = 1000 J/(kg·K), J_f = 0.27 kg/(m^2·s), p = 10^5 Pa, T_0 = 20 °C, T_{mf} = 327 °C, T_{mb} = 423 °C, (γ =1.16), Q = 130·10^3 W/m^2, ($Q > J_f c_f (T_{mb} - T_0)$ = 109·10^3 W/m^2).

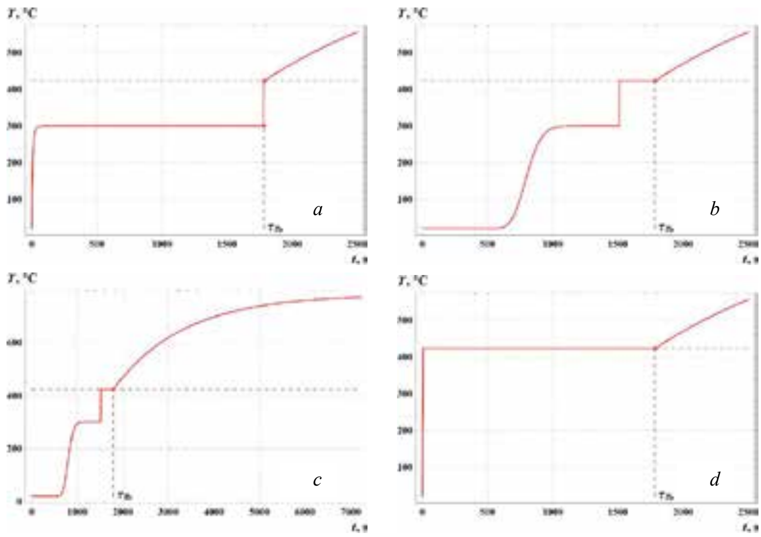

Fig. 2. Bed temperature dependence on time in different horizontal cross sections.
(0 (*a*), $H/2$ (*b*), $H/2$ for $t \in [0, \tau_\Sigma]$ (*c*), H (*d*)). The rest of parameters are the same as for Fig.1.

The asymptotic value of T_{fb} is:

$$T_{fb}(\infty) = T^0 + \frac{Q}{c_f J_f}. \qquad (12)$$

The bed heating time is $\tau_\Sigma = \tau_{fb} + \tau_{fb}^*$, where τ_{fb}^* determined from (11) provided $T_{fb}(\tau_\Sigma) = 0.99\, T_{fb}(\infty)$ as

$$\tau_{fb}^* = -\frac{c_s \rho_s (1-\varepsilon) H}{c_f J_f} \ln\left(\frac{0.01(T^0 + Q/(c_f J_f))}{T^0 + Q/(c_f J_f) - T_{mb}}\right). \qquad (13)$$

Fig. 3 and 4 shows the temperature distribution provided $T^0 > T_{mb}$. In this case, apparently, the transition front of a fixed bed in the fluidized bed passes through only part of initial bed height. A feature of the temperature distribution along the bed height (Fig. 3) is the presence within it of low temperature region, which is "collapsing" in time moment τ_{fb} at coordinate h_*, where $T_{gb} = T_{mb}$ (Fig. 3*c*). At time τ_{fb} by intensive mixing of the particle bed temperature is leveled over its entire height to a value of $<T>$:

$$<T> = h_* <T_{gb}> + (H - h_*) T_{mb}, \qquad (14)$$

where $<T_{gb}> = \frac{1}{h_*}\int_0^{h_*} T_{gb}(\tau_{fb}, x)\,dx$.

When $t > \tau_{fb}$, the exponential heating of fluidized bed starts (Fig. 4) in accordance with equation (11), wherein T_{mb} to be replaced by the average temperature $<T>$, determined from (14).

As seen from a comparison of Figs. 1 and 3, the position where the fronts of top and bottom heating meet, practically does not depend on T^0. Its value $x \sim 0.3$ m indicates that the rate of heat wave for the lower heating almost three times exceed the transfer speed of the front "fixed - fluidized bed" for the top one.

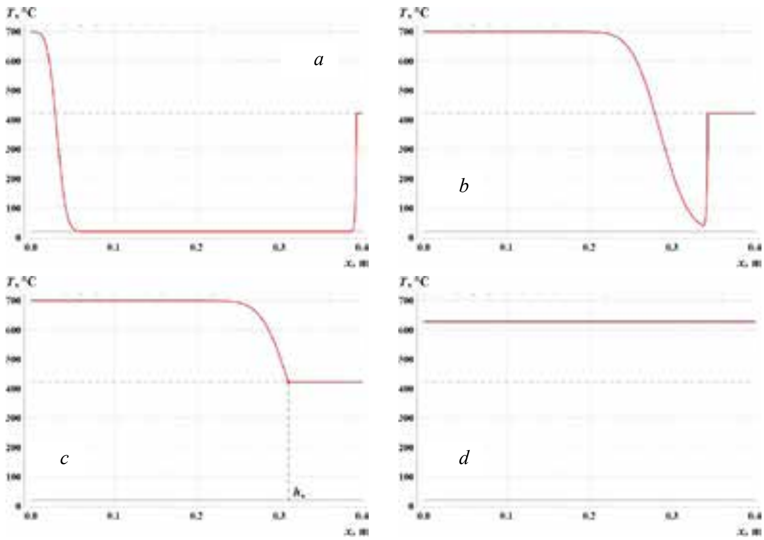

Fig.3. Temperature distributions along the bed height in different time moments. T^0 = 700 ºC, τ_{fb} = 1300 s. ($0.1\cdot\tau_{fb}$ (*a*), $0.9\cdot\tau_{fb}$ (*b*), τ_{fb} (*c*), $1.01\cdot\tau_{fb}$ (*d*)). The rest of parameters are the same as for Fig.1.

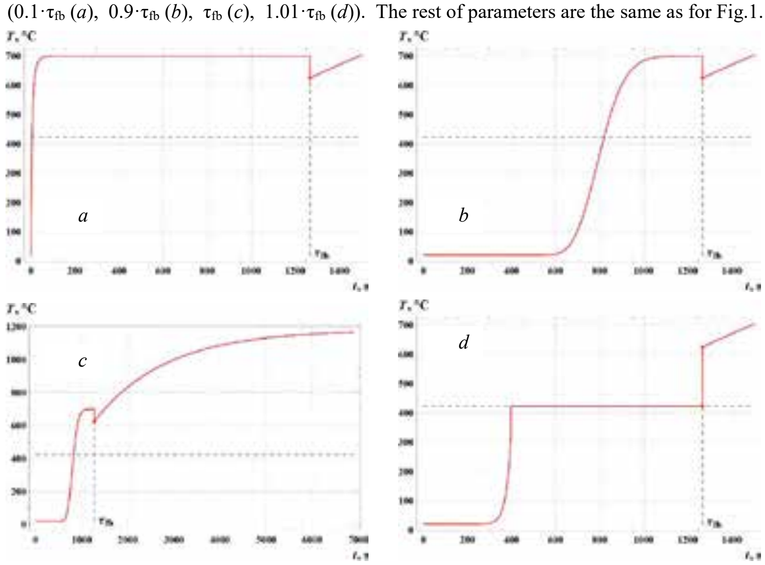

Fig. 4. Bed temperature dependence on the time in different horizontal cross sections. T^0 = 700 ºC τ_{fb} = 1300 s. (0 (*a*) , *H*/2 (*b*), *H*/2 for $t \in [0, \tau_\Sigma]$ (*c*), 0.95*H* (*d*)). The rest of parameters are the same as for Fig.1.

Fig. 5 shows the dependences $h(t)$ for the top (*a*) and the combined (*b*, *c*) heating. As can be seen, the complete bed fluidization time τ_{fb} essentially depends on the value of T^0. In the case of $T^0 < T_{mb}$ (Fig. 5*b*) the transition "fixed - fluidized bed" front rate increases significantly in the region $t \sim t_* = 1450$ s, while the temperature of the bed before the front approaches the T^0 (Fig. 1*b*).

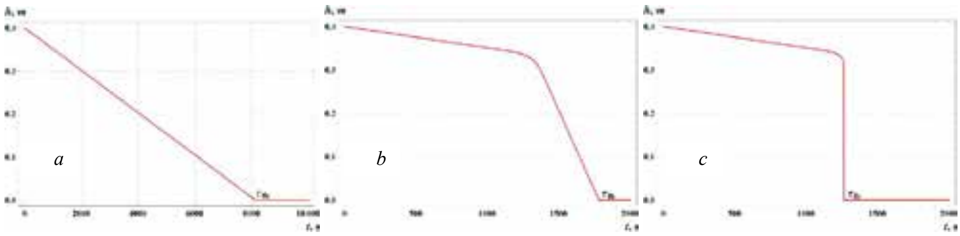

Fig. 5. The position of the transition “fixed – fluidized” bed front h dependence from time for:
T^0 = 20 ºC (upper heating) (*a*), T^0 = 300 ºC (*b*), T^0 = 700 ºC (*c*). The rest of parameters are the same as for Fig.1.

EFFICIENCY OF KINDLING PROCESS

Ignoring the heat exchange of the granular bed with the walls, kindling efficiency η can be defined as the ratio of the amount of heat going to heat the bed to the total amount of heat supplied to the bed. For comparison, consider the cases of the upper and lower heating during τ_{fb} time.

a). A lower heating. From the heat balance equation

$$c_s\rho_s(1-\varepsilon)H(T_{mb}-T_0)=\int_0^{\tau_{fb}} c_f J_f (T^0 - T_{gb}(t,H))dt \qquad (15)$$

one obtains for η:

$$\eta=\frac{c_s\rho_s(1-\varepsilon)H(T_{mb}-T_0)}{c_f J_f(T^0-T_0)\tau_{fb}}=\frac{1}{\tau_{fb}}\int_0^{\tau_{fb}}\frac{T^0-T_{gb}(t,H)}{T^0-T_0}dt\,. \qquad (16)$$

The output temperature of the bed $T_{gb}(t, H)$ is determined from the solution of (1) – (4), (7).

b). An upper heating. The balance equation provided $T^0 = T_0$ has the form of

$$c_s\rho_s(1-\varepsilon)H(T_{mb}-T_0)=(Q-c_f J_f(T_{mb}-T_0))\tau_{fb}\,. \qquad (17)$$

Using (8) we obtain the

$$\eta=\frac{c_s\rho_s(1-\varepsilon)H(T_{mb}-T_0)}{Q\tau_{fb}}=1-\frac{c_f J_f(T_{mb}-T_0)}{Q}\,. \qquad (18)$$

Fig. 6 shows a comparison of the values η, calculated according to (16) and (18). The minimum value of Q for each chart is determined by the achievement of boiling for the upper heating ($Q_{min}=c_f J_f(T_{mb}-T_0)$), and the maximum – compliance T^0 = 800 ºC for the lower ($Q_{max}=c_f J_f(T^0-T_0)$). As can be seen, the lower kindling efficiency is substantially higher than the upper one because of the large heat losses from exhaust gases. As a result, the total time of heating the bed at the lower kindling is significantly lower than at the upper one.

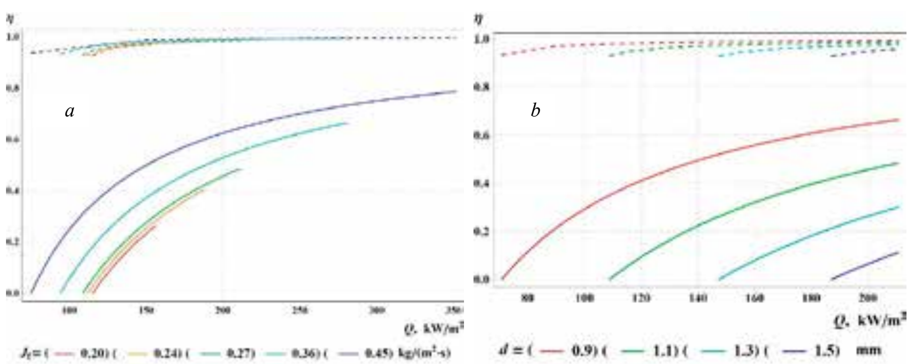

Fig. 6. Comparing the efficiency of heating η dependences from Q for the lower (dashed lines) and upper (solid lines) heating with different J_f (*a*) and d (*b*). The rest of parameters are the same as for Fig.1.

THE CALCULATION OF THE MINIMAL HEAT FLOW REQUIRED FOR THE FLUIDIZATION OF THE BED

The calculation of this value is carried out according to the dependence

$$Q_{\min} = c_f J_f (\gamma T_{mf} - T_0), \tag{19}$$

where temperature T_{mf} is calculated based on the well-known Todes formula for the minimum fluidization velocity from the transcendental equation for atmospheric pressure conditions:

$$J_f = \rho_f(T_{mf}) \frac{\nu_f(T_{mf})}{d} \frac{\mathrm{Ar}(T_{mf})}{1400 + 5.22\sqrt{\mathrm{Ar}(T_{mf})}}. \tag{20}$$

Fig. 7 shows the function of $Q_{\min}(J_f, d)$. It is clearly seen that at low airflows the Q value required for fluidization increases significantly (for the small particles especially).

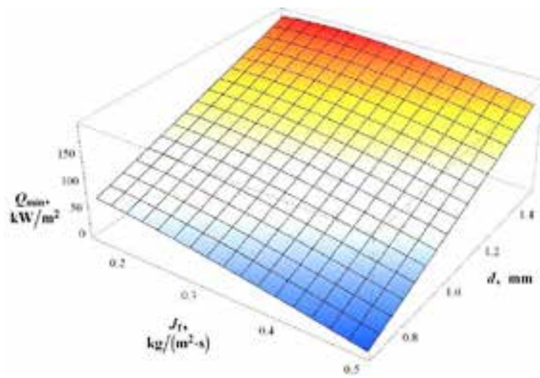

Fig. 7. A surface plot of the function $Q_{\min}(J_f, d)$. The rest of parameters are the same as for Fig.1.

EXPERIMENTAL STUDY

The process of upper heating of the fluidized bed was investigated on the operational boiler with capacity 0.5 MW (Fig. 8).

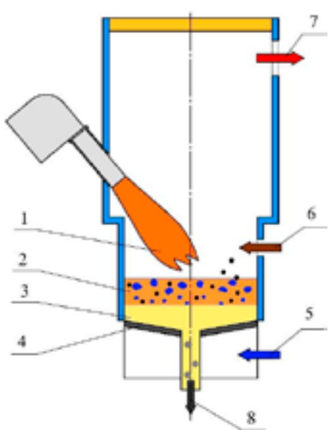

Fig. 8. Scheme of the boiler with capacity of 0.5 MW. 1 – flame of burner; 2 – the fluidized bed, composed of inert material; 3 – the fixed bed, composed of inert material; 4 – gas distribution grid; 5 – primary air supply; 6 – solid fuel supply; 7 – removal of burning products; 8 – removal of slag formations.

Quartz and olivine sand with an average diameter of 0.59 and 0.31 mm respectively was used as inert material. Velocity of fluidization was u_{mf} = 0.23 and 0.09 m/s, respectively. The bed height was varied in the range of H = 200 ÷ 300 mm. The inner diameter of the fluidized bed was 850 mm.

Ignition algorithm was as follows:

a) turning on primary fan supplying air at $u \approx u_{mf}$ ($T_{mf} = T^0 \approx 20$ °C);
b) turning on the burner and the fuel supply auger;
c) when fuel has been ignited, supply of primary air was increased until the visual observation of individual breakthroughs air jets;
d) upon reaching the bed temperature of 250 – 300 °C fuel supply was turned off;
e) at a temperature of 700 ÷ 750 °C the burner was turned off.

Note that the use of fuel during ignition is needed due to the insufficient capacity of the burner (~ 200 kW).

Experimental dependences of $T(t, 0)$, measured by the three thermometers are shown in Fig. 9.

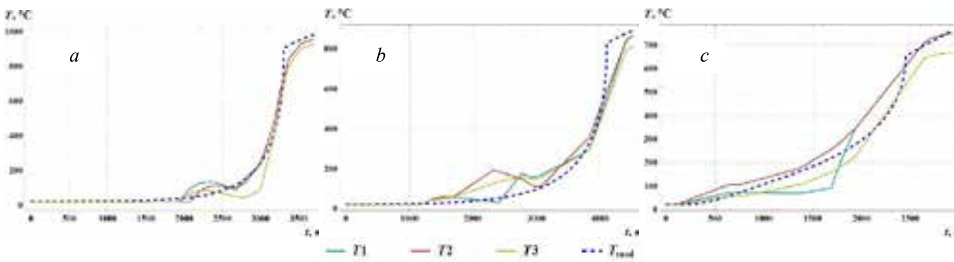

Fig. 9. The time dependence of temperature at the input of granular bed. $T1$ – temperature at the bottom of bed (above the grid) in 33 cm from the wall, $T2$ – in 16 cm, $T3$ – in 9 cm, T_{mod} – the result of $T(t, 0)$ calculation according to the model used. *a* – quartz sand, straw pellets: λ_{gb} = 8 W/(m·K), J_f = 0.27 kg/(m²·s) Q = 288 кW/m², τ_{gb} = 3300 s; *b* – quartz sand, kindlings, λ_{gb} = 16 W/(m·K), J_f = 0.27 kg/(m²·s) Q = 272 кW/m², τ_{gb} = 4100 s; *c* – olivine sand, straws, λ_{gb} = 27 W/(m·K), J_f = 0.11 kg/(m²·s) Q = 158 кW/m², τ_{gb} = 2400 s.

As one can see, in these conditions, a fluidized bed boiler ignition includes a set of operations, direct accounting of which in the framework of the developed mathematical model is a non-trivial task. To solve it, we note that at the beginning of kindling a bed was fluidized weakly ($u = u_{mf} + o$). This allows the presence of macroscopic motion of the particles, which could lead to a significant increase in longitudinal thermal conductivity of the bed as compared to its value for the granular bed ($\lambda_0 + 0.5c_f J_f d$).In this regard, the particular choice of the value of λ_{gb} was carried out by comparing the calculated and experimental dependences $T(t, 0)$. The current value of Q assumed to be constant and determined by the formula (8), taking into account the experimental values τ_{fb} and T_{mb}. Fig. 9 shows a comparison of experimental curves $T(t, 0)$ with calculated by means of (1) – (5) ones. As can be seen, mathematical model, used for the description of the granular bed heating, allows to describe the dynamics of the process good enough even with complicated performance of it.

CONCLUSION

As a result of modeling the combined heating of the granular bed, dependences of the time of heating from defining parameters established ((8), (13)). It is shown that the efficiency of the lower heating is higher in comparison with the upper heating, because of the large losses of heat from outgoing gas having a maximum temperature in the latter case. The dynamics of heating the granular bed of quartz and olivine sand in the furnace of the boiler capacity of 0.5 MW is investigated. It is shown that the model (1) – (5) by using reasonable assumptions allows well enough to describe the observed experimental dependence of $T(t, 0)$.

ACKNOWLEDGMENT

This work was supported by the Belarusian Republican Foundation for Fundamental Research.

NOTATION

Ar Archimedes number ($\mathrm{Ar} = gd^3(\rho_s/\rho_f - 1)/\nu_f^2$)
c_f, c_s specific heat of gas and particles, respectively J/(kg·K)
d diameter of particles, m
g gravitational acceleration, m/s^2
h position of the fluidized and fixed bed sections interface, m
H height of the granular bed, m
$J_f = \rho_f u$ mass flow rate of gas, kg/(m^2·s)
Q heat flow density, W/m^2
t time, s
T temperature, K
T_{gb}, T_{fb} fixed and fluidized beds temperatures, K
T_0 initial temperature of granular bed, K
T^0 inlet temperature of gas, K
u gas superficial velocity, m/s
u_{mf} minimum fluidization velocity, m/s
u_{mb} minimum velocity of bubbling fluidization, m/s
x longitudinal coordinate, m
ε porosity
$\gamma = T_{mb}/T_{mf}$
λ_{gb} longitudinal thermal conductivity of the fixed bed, W/(m·K) ($\lambda_{gb} = \lambda_0 + 0.5c_f J_f d$)
λ_0 thermal conductivity of not filtered granular bed, W/(m·K)
ν_f kinematic viscosity of the gas, m^2/s
ρ_f, ρ_s density of gas and particles, respectively kg/m^3
τ_{fb} time required for complete fluidization of the bed, s
τ_{fb}^* heating time of the fully fluidized bed, s

The subscripts:

f gas
gb granular (fixed) bed
fb fluidized bed
mb minimum velocity of bubbling fluidization
mf minimum fluidization
min minimum
s particles
Σ total

REFERENCES

Chermalyh G. N., Mahorin K. E. 1965. Radiation heating of the fluidized bed. Journal of Engineering and Physics, V. 15, N. 3, pp. 477-480.

Keler V. R., Podshivalov V. G., Berg B. V. 1989. Kindling the apparatuses with fluidized bed using liquid fuel. Proceeding “Problems of heat and mass transfer in a modern technology of combustion and gasification of solid fuels” Heat and Mass Transfer Institute, National Academy of Sciences of Belarus, Minsk, Belarus, pp. 17-19.

Pitsukha E. A., Teplitskii A. I., Roslik A. R. 2016. About the thermal fluidization of granular bed in case upper heating. Journal of Engineering and Physics (in publishing).

Protsailo M. Y., Yangolov O. V., Shchipko M. L. et al. 1991. Features ignition fluidized bed boilers using the Kansk-Achinsk coals. Thermal Engineering, N. 3, pp. 19-22.

Richardson J. F. 1974. A beginning of fluidization and the homogeneous systems. Proceeding “Fluidisation” edited by Davidson I. F. and Harris, Moscow, pp. 37-73.

Ruzhnikov S. G., Tarasov E. P., Shchipko M. L. et al. 1988. Analysis of the process of launching a fluidized bed boiler. Proceedings “Heat and Mass Transfer – MMF”, Heat and Mass Transfer Institute, National Academy of Sciences of Belarus, Minsk, Belarus, Sec. 10, pp. 85-87.

Shteiner I. N., Rassudov N. S., Gollbraih I. S. et al. 1985. Ignition fuel and kindling fluidized bed firing installations. Thermal Engineering, N. 5, pp. 32-35.

Zabrodski S. S., 1971. High temperature plants with the fluidized bed. Energy, Moscow.